*The definitive version was published in Science, **2023**, 382, 325-329, DOI: 10.1126/science.adj7007.*

*https://science.org/doi/10.1126/science.adj7007*

# Taming Secondary Benzylic Cations in Catalytic Asymmetric $S_N1$ Reactions

Vikas Kumar Singh[1†], Chendan Zhu[1†], Chandra Kanta De[1†], Markus Leutzsch[1], Lorenzo Baldinelli[2], Raja Mitra[3], Giovanni Bistoni[2], and Benjamin List[1*]

[1]Max-Planck-Institut für Kohlenforschung, Kaiser-Wilhelm-Platz 1, D-45470 Mülheim an der Ruhr, Germany.

[2]University of Perugia, Department of Chemistry, Biology and Biotechnology, 06122 Perugia, Italy.

[3]School of Chemical and Materials Sciences, Indian Institute of Technology, Farmagudi, Ponda, Goa-403401.

*Corresponding author. Email: list@kofo.mpg.de

†These authors contributed equally to this work.

**Abstract:** Benzylic stereogenic centers are ubiquitous in natural products and pharmaceuticals. A potentially general though challenging approach toward their selective creation would be asymmetric $S_N1$ reactions that proceed through highly reactive benzylic cations. We now report a broadly applicable solution to this problem by identifying chiral counteranions that pair with secondary benzylic cations to engage in catalytic asymmetric C–C-, C–O- and C–N-bond forming reactions with excellent enantioselectivity. The critical cationic intermediate can be accessed from different precursors *via* Lewis- or Brønsted acid catalysis. Key to our strategy is the use of only weakly basic, confined counteranions that are posited to prolong the lifetime of the carbocation, avoiding non-productive deprotonation pathways to the corresponding styrene.

**One-Sentence Summary:** Confined and weakly basic counteranions pair with secondary benzylic cations to engage in catalytic asymmetric C–C-, C–O- and C–N bond forming $S_N1$ reactions with excellent enantioselectivity.

**Main Text:** Benzylic stereocenters are omnipresent substructures of a vast number of natural products and drugs (*1*). For the asymmetric construction of the crucial benzylic C–C or C–heteroatom bond, a plethora of methods has been described. Approaches using chiral auxiliaries, metal catalysts, organocatalysts, and enzymes, among others, are known (*2–5*). However, despite potential as a general approach to benzylic stereocenters, the catalytic enantioselective reaction of a nucleophile with a benzylic cation remains underdeveloped. During the past decade, early attempts towards this strategy have been reported but typically involved oxygenated arenes, stabilizing the corresponding benzylic cation as *ortho*- or *para*-quinone methides and thus limiting the scope of these methods (*6–12*).

**Fig. 1. Subjecting benzylic cations to asymmetric catalysis.** (**A**) Dynamic kinetic asymmetric transformations *via* benzylic cations. (**B**) This work: confined counteranions tame secondary benzylic cations for asymmetric catalysis.

Recently, the Jacobsen group reported an allylation of tertiary benzylic cations for the construction of quaternary stereogenic centers using anion-binding, hydrogen bond-donor catalysis (Fig. 1A) (*13*). Subsequently, the Sun group explored tertiary benzylic cations as intermediates in asymmetric catalysis (*14*). Asymmetric catalysis of reactions proceeding through unstabilized secondary benzylic cations has previously been reported by the Braun and Toste groups, albeit each with only a single example (Fig. 1A) (*15*, *16*). We hypothesized that engaging unbiased secondary benzylic carbocationic intermediates with a wide range of nucleophiles could provide a general solution to the problem of constructing benzylic stereocenters (Fig. 1B).

Over the past years, highly acidic and enzyme-like confined imidodiphosphorimidates (IDPi) catalysts have emerged as a powerful motif to control the enantioselectivity in the reactions of high-energy, cationic intermediates such as tertiary benzylic carbocations, vinyl carbocations and the non-classical 2-norbornyl cation (*17–20*). Initially, we expected three fundamental challenges toward applying our design to unstabilized secondary benzylic cations: (i)the differentiation between two faces of an only hydrocarbon-based planar cationic intermediate , (ii) the exclusion of unproductive reaction pathways such as deprotonation or rearrangement, and (iii) potential catalyst deactivation by alkylation from the benzylic cation. Given the high local electrophilicity and hydride ion affinities of benzylic cations, we postulated that essential cation stabilization could

be achieved using a less basic, weakly coordinating anion, which at the same time can also provide a chiral microenvironment for further nucleophilic attack to achieve high enantiocontrol (*21–23*).

Here we report the design and development of an IDPi catalyzed $S_N1$ platform that enables the conversion of racemic $sp^3$ starting materials into valuable enantioenriched benzylic stereocenter-containing products in a dynamic kinetic asymmetric transformation.

**Reaction development.** First, we explored C–O bond forming reactions between *rac*-1-phenylethyl 2,2,2-trichloroacetimidate (**1a**) as the cation precursor and acetic acid as the nucleophile in the presence of different IDPi catalysts. In the initial attempts, we found an IDPi catalyst (**S2h**) could catalyze this reaction, giving the desired product **3a** in 86% yield with 61:39 enantiomeric ratio (er), so further optimizations were carried out (see supplementary materials for details). Eventually, IDPi **2a** was identified as the optimal catalyst, delivering product **3a** in 73% yield and with 95:5 er (Fig. 2A). With the optimal conditions (IDPi 2a, T = –90 °C, t = 5 d) established, we turned our attention toward exploring the scope for this transformation. Substrates (**1b–d**) with *meta* or *para* substituents performed well and furnished the products with high enantioselectivities and modest to good yields. When propionic acid was employed as the nucleophile, fluorenyl substituted IDPi catalyst **2b** demonstrated superior performance. Propionate products **3e**–**h** were obtained in good yields and with high enantioselectivities.

**Fig. 2. Substrate scope of the Brønsted acid catalyzed C–O and C–N bond forming reactions.** (**A**) C–O bond formation reaction. (**B**) C–N bond formation reaction. See supplementary materials for details. er = enantiomeric ratio. Tf = $SO_2CF_3$. Nf = $–SO_2C_4F_9$. Hdf = $–SO_2C_8F_{17}$. $Et_2O$ = diethyl ether. Ph = phenyl. Et = ethyl. Pr = propyl. Bu = butyl.

These results are consistent with a facile ionization of trichloroacetimidate **1a**, even at low temperature, delivering the highly reactive benzylic carbocation along with trichloroacetamide. We wondered if the *in situ* generated trichloroacetamide could itself act as an *N*-nucleophile in the absence of an external *O*-nucleophile. Such reaction might serve as an attractive approach to the enantioselective formation of benzylic C–N bonds from benzylic alcohols (*24–28*). However, trichloroacetamide is only poorly soluble in diethyl ether at low temperature, and an undesired deprotonation to styrene could be problematic. Indeed, upon testing various IDPi catalysts, the desired rearrangement product **4a** was obtained with moderate to good enantioselectivities but in only poor yield with significant amounts of styrene as side product (See supplementary materials

for details). We reasoned that the undesired deprotonation pathway could be minimized by using even less basic IDPi counteranions, requiring more acidic IDPi catalysts. As shown in our previous work, electron-withdrawing groups on the BINOL backbone enhance the acidity of IDPi catalysts (*29*). Therefore, attempts to diminish the deprotonation pathway were made by modulating the electronic properties of the catalyst. Gratifyingly, $F_8$-substitution of one BINOL skeleton led to catalyst **2c**, which provided the desired product **4a** in 75% yield and with an excellent 95:5 enantiomeric ratio (Fig. 2B). Moreover, substrates **1b–e** bearing alkyl groups and halogen atoms at the *meta* or *para* positions provided the corresponding products with good to excellent enantioselectivities and moderate to good yields using catalyst **2d**.

**Extension to carbon nucleophiles.** With the successful implementation of these Brønsted acid catalyzed asymmetric C–O and C–N bond forming $S_N1$ reactions, we were keen on exploring the exciting potential to create C–C bonds by a similar pathway. We envisioned the previously unknown reactions of secondary benzylic alcohol derivatives with silyl ketene acetals or electron rich arenes toward the formation of β-branched esters or 1,1-diaryl ethanes, respectively, as particularly attractive targets. A somewhat related copper catalyzed enantioselective substitution of benzylic propargylic acetates using indoles has been described (*30*). However, with silyl ketene acetal, only 10% yield and no enantioinduction was obtained. Similarly, our initial attempts at reacting trichloroacetimidate **1a** with silyl ketene acetals (SKA) using IDPi catalysts did not lead to the desired C–C-bond forming product and only the substrate **1a** was recovered. We speculate that imidate **1a** engages in a deprotosilylation (*31*), the product of which however is unreactive toward ionization to the reactive benzylic carbocation. We had previously shown that heteroatom stabilized cations (oxocarbenium ions and iminium ions) can be generated under (oxophilic) silylium Lewis acid catalysis conditions when acetate was employed as leaving group (*32*). We therefore investigated racemic 1-phenylethyl acetate (**5a**) as substrate toward a silylium-Lewis acid catalyzed cation formation. Indeed when acetate **5a** was treated with ((1-(benzyloxy)vinyl)oxy)(tert-butyl)dimethylsilane (**8a**) in the presence of IDPi catalysts, the desired product **6a** was obtained in good yields and with moderate to good enantioselectivities (See supplementary materials for details). Upon optimization, we found that IDPi catalyst **2e** provided product **6a** with an er of 92.5:7.5 and in 85% yield (Fig. 3A). Other substrates with alkyl substituents at the *para* position, linear or branched and with different chain lengths, delivered products **6b–f** in 84–91% yields with high enantioselectivities using fluorenyl substituted IDPi

catalyst **2f**. Substrate **5g** having *meta*, *para* disubstitution furnished product **6g** in 92% yield with 95:5 er. Furthermore, product **6h** was obtained with modest enantioselectivity using catalyst **2e** where a methoxy group in place of acetate was employed as leaving group for substrate **5h** since the corresponding acetate substrate was found to be unstable for isolation. The microenvironment of the binding site in the IDPi catalyst allows the C–C bond formation to proceed by selective addition of a single SKA nucleophile. Presumably, the steric differentiation between substrate and the product prevents the product from participating further in a Mukaiyama–Claisen-type condensation reaction.

**Fig. 3. Substrate scope of the silylium Lewis acid catalyzed C–C-bond forming reactions.** (**A**) SKA α-alkylation reaction. (**B**) Friedel–Crafts reaction. See supplementary materials for details. er = enantiomeric ratio. Tf = $–SO_2CF_3$. Nf = $–SO_2C_4F_9$. Hdf = $–SO_2C_8F_{17}$. $Et_2O$ = diethyl ether. TBSO = tert-butyldimethylsilyloxy. TMSO = trimethylsilyloxy. Bn = benzyl. OMe = methoxy. Ac = acetyl. BSTFA = *N*,*O*-bis(trimethylsilyl)trifluoroacetamide.

**Asymmetric Friedel-Crafts alkylations.** With the successful establishment of a silylium Lewis acid catalyzed C–C-bond forming $\alpha$-alkylation reaction, we were keen to expand the asymmetric transformation of secondary benzylic cations with other C–nucleophiles. The Friedel–Crafts alkylation as a classic and broadly applicable transformation proceeding via carbocations became a natural target. Previously, asymmetric catalytic Friedel–Crafts alkylations involving benzylic cations had not been reported. Compared to carboxylic acids and SKAs, electron-rich arenes are much weaker nucleophiles (*33, 34*). We therefore envisioned controlling and stabilizing the benzylic cation in this electrophilic aromatic substitution reaction a rather challenging task. Gratifyingly, under silylium Lewis acid conditions, the Friedel–Crafts alkylation of racemic acetate substrate **5a** with anisole gave product **7a** in 60% yield with 96:4 er and > 50:1 regioisomeric ratio (rr) using IDPi catalyst **2g** (Fig. 3B). Different anisoles were evaluated under these conditions with the same catalyst. When anisoles with *ortho* and *meta* substituents were applied in this transformation, products **7b** and **7c** were obtained with excellent enantioselectivities, regioselectivity and modest yields. Notably, a silylated phenol was found to be a suitable nucleophile for this transformation and delivered the trimethylsilylated product **7d** in good yield with high enantioselectivity. Furthermore, this conversion also proceeded under purely Brønsted

acid catalytic conditions using substrate **1a** and the same IDPi catalyst **2g** to furnish the same product with consistent enantioselectivity, in line with the formation of a benzylic cation *via* $S_N1$ reaction (See supplementary materials for details).

**Fig. 4. Mechanistic studies, characterization of ion pair and origin of enantioselectivity** (**A**) Proposed reaction pathway. (**B**) Enantioselectivity and NMR yield comparison of *rac*-**1a** with enantiopure **1a** substrate. (**C**) Reactivity measurements of *rac*-**1a** and enantiopure **1a**; reaction monitored by $^1$H NMR at –60 °C. (**D**) $^1$H NMR spectrum of ion pair (**9**) consisting of 1-(2,4,6-trimethoxyphenyl)ethan-1-ylium cation and bistriflimide anion. (**E**) $^{13}$C NMR spectrum of ion pair (**9**). (**F**) Comparison of HSQC spectrum for bistriflimide and IDPi (**S2h**) anions. (**G**) DFT optimized ion pair structure. (**H**) Electrostatic potential map (MEP) of ion pair. (**I**) Topographic steric map of the ion pair (see supplementary materials for orientation and further details).

**Mechanistic considerations.** Experimental and computational studies were carried out to challenge our benzylic cation $S_N1$–hypothesis (Fig. 4A). At first, substrate *rac*-**1a** and each of the enantiopure starting materials, (*S*)-**1a** or (*R*)-**1a**, were individually subjected to the optimized reaction conditions. Consistent with the ion pair formation followed by nucleophilic attack on the benzylic cation in a $S_N1$ like mechanism, we found that all three reactions delivered the same major enantiomer of product **3a** with essentially identical yield (85%, 86%, and 85%, by NMR) and enantioselectivity (95:5, 95:5, and 94.5:5.5 er) (Fig. 4B). Interestingly, when the progress of the C–O bond forming reaction was monitored by $^1$H NMR at –60 °C for each substrate separately (*rac*-**1a**, enantiopure (*S*)-**1a**, and (*R*)-**1a**), both enantiomers were found to react with similar rates showing very little to no kinetic resolution (Fig. 4C). Attempts to characterize either an ion pair or a covalent adduct in the reaction of substrate **1a** with IDPi **2a** were unsuccessful, exclusively delivering product **4a** and styrene under the reaction conditions. To gain further insight into the cationic intermediates and their lifetime, we investigated a series of biased substrates featuring different substitution patterns, which were ionized with $HNTf_2$ as strong achiral acid. In most cases, the ion pair was either not detectable or it rapidly underwent decomposition during the measurement (see supplementary materials for details). We anticipated the ion pair resulting from the reaction of 1-(2,4,6-trimethoxyphenyl)ethan-1-ol (**5i**) and $HNTf_2$ to have a sufficiently long lifetime for its characterization. Indeed, when alcohol **5i** was treated with $HNTf_2$ (3 equiv.) in

$CD_2Cl_2$ at –60 °C in an NMR tube, the formation of the ion pair was observed and could be characterized by NMR spectroscopy ($^1H$, $^{13}C$ and 2D NMR experiments) (Fig. 4D, 4E). A gradual increase of the temperature from –60 °C to –20 °C was performed and the resulting mixture was monitored by NMR spectroscopy. Ion pair **9** was found to be stable in that range and only start to decompose at higher temperature. The same ion pair **9** could also be generated under silylium Lewis acid conditions and a similar behavior was observed in this case (see supplementary materials for details). Importantly, the oxygenated benzylic cation could also be observed with catalyst **S2h** in NMR experiments. Decomposition of this ion pair species **10** was observed at –60 °C presumably due to the relatively higher basicity of the IDPi counteranion compared to the $NTf_2$ anion. A shift in the $^1H$ and $^{13}C$ NMR (benzylic proton from 8.7 to 8.5 ppm and benzylic carbon from 173.8 to 172.8 ppm) was observed (Fig. 4F), clearly indicating different counteranions in the close proximity of the cation. In addition, density functional theory (DFT) was used to optimize the ion-pair. A large number of conformers was initially generated at various levels of GFNn-FF/XTB theory, and the low-energy structures were refined using DFT (see supplementary materials for details). Analysis of the electrostatic potential surfaces reveals that the ion pair structure is held together by directional electrostatic interactions between the IDPi anion and the benzylic carbocation (Fig. 4G–4I). The computed association free energy between the IDPi anion and benzylic carbocation ($\Delta G$) is negative (-22.08 kcal/mol), indicating that the formation of the ion pair is thermodynamically favored. The decomposition of the electronic interaction energy between the anion and the cation ($\Delta E_{int}$ = -43.21 kcal/mol) into dispersive ($\Delta E_{disp}$) and steric/electrostatic components ($\Delta E_{ster/elec}$) shows that dispersion plays a crucial role in favoring the formation of the chiral ion pair, contributing with 27.33 kcal/mol to $\Delta E_{int}$. The negative interaction is at least partially counterbalanced by: (i) the energy penalty required to distort the catalyst to maximize the electrostatic interaction with the cation and (ii) entropy and temperature effects. Most notably, the cation resides between the 3-biphenyl substituents of the BINOL skeleton (3.6 Å and 3.2 Å, respectively) that aid in stabilizing the reactive intermediate by virtue of cation–π interactions. Additionally, the benzylic CH group clearly interacts with a sulfonyl oxygen atom (2.2 Å), as well as the phenyl 3-CH with an inner core nitrogen atom (2.34 Å, for a full display of interactions see fig. S6). It is plausible to assume that all of these interactions can be expected to play a vital role in the stabilization of the respective transition states leading to the major enantiomer.

Given the significance of carbocations in chemical synthesis, our results may have broader implications for a plethora of other fundamental organic transformations.

**References and Notes**


1. N. A. McGrath, M. Brichacek, J. T. Njardarson, A graphical journey of innovative organic architectures that have improved our lives. *J. Chem. Educ.* **87**, 1348–1349, (2010).
2. G. C. Fu, Transition-Metal catalysis of nucleophilic substitution reactions: a radical alternative to $S_N1$ and $S_N2$ processes. *ACS Cent. Sci.* **3**, 692–700, (2017).
3. D. T. Ziegler, G. C. Fu, Catalytic enantioselective carbon−oxygen bond formation: Phosphine−catalyzed synthesis of benzylic ethers *via* the oxidation of benzylic C−H bonds. *J. Am. Chem. Soc.* **138**, 12069−12072, (2016).
4. Chapter 4: Engineering Enzymes for New-to-Nature Carbene Chemistry" S. Athavale, K. Chen, F. H. Arnold. In transition metal−catalyzed carbene transformations DOI: 10.1002/9783527829170.ch4.
5. M. D. Ennis, D. J. Mathre, D. A. Evans, Asymmetric alkylation reactions of chiral imide enolates. A practical approach to the enantioselective synthesis of α-substituted carboxylic acid derivatives. *J. Am. Chem. Soc.* **104**, 1737−1739, (1982).
6. Z. Wang, J. Sun, Recent advances in catalytic asymmetric reactions of *o*−quinone methides. *Synthesis* **47**, 3629–3644, (2015).
7. A. A. Jaworski, K. A. Scheidt, Emerging roles of *in situ* generated quinone methides in metal-free catalysis. *J. Org. Chem.* **81**, 10145−10153, (2016).
8. W. Li, X. Xu, P. Zhang, P. Li, Recent advances in the catalytic enantioselective reactions of *para*−quinone methides. *Chem. Asian. J.* **13**, 2350−2359, (2018).
9. J. Kikuchi, M. Terada, Enantioconvergent substitution reactions of racemic electrophiles by organocatalysis. *Chem. Eur. J.* **27**, 10215–10225, (2021).
10. C. Dorsch, C. Schneider, Asymmetric Brønsted acid catalyzed cycloadditions of *ortho*−quinone methides and related compounds. *Synthesis* **54**, 3125−3141, (2022).
11. X. Li, Z. Li, J. Sun, Quinone methides and indole imine methides as intermediates in enantioselective catalysis. *Nat. Synth.* **1**, 426–438, (2022).
12. J. Ouyang, R. Maji, M. Leutzsch, B. Mitschke, B. List, Design of an organocatalytic asymmetric (4 + 3) cycloaddition of 2-indolylalcohols with dienolsilanes. *J. Am. Chem. Soc.* **144**, 8460–8466, (2022)
13. A. E. Wendlandt, P. Vangal, E. N. Jacobsen, Quaternary stereocentres *via* an enantioconvergent catalytic $S_N1$ reaction. *Nature* **556**, 447–451, (2018).
14. X. Tan, Z. Deng, Q. Wang, S. Chen, G. Zhu, J. Sun, Enantioselective synthesis of tetraarylmethanes through meta-hydroxyl-directed benzylic substitution. *Nat. Synth.* s44160-022-00211-4 (2023).
15. M. Braun, W. Kotter, Titanium(IV)−catalyzed dynamic kinetic asymmetric transformation of alcohols, silyl ethers, and acetals under carbon allylation. *Angew. Chem. Int. Ed.* **43**, 514–517, (2004).
16. C. Zhao, F. D. Toste, K. N. Raymond, R. G. Bergman, Nucleophilic substitution catalyzed by a supramolecular cavity proceeds with retention of absolute stereochemistry. *J. Am. Chem. Soc.* **136**, 14409–14412, (2014).

17. N. Tsuji, J. L. Kennemur, T. Buyck, S. Lee, S. Prévost, P. S. J. Kaib, D. Bykov, C. Farès, B. List, Activation of olefins *via* asymmetric Brønsted acid catalysis. *Science* ***359***, 1501−1505, (2018).

18. P. Zhang, N. Tsuji, J. Ouyang, B. List, Strong and confined acids catalyze asymmetric intramolecular hydroarylations of unactivated olefins with indoles. *J. Am. Chem. Soc.* **143**, 675–680, (2021).

19. R. Properzi, P. S. J. Kaib, M. Leutzsch,G. Pupo, R. Mitra, C. K. De, L. Song, P. R. Schreiner, B. List, Catalytic enantiocontrol over a non-classical carbocation. *Nat. Chem.* **12**, 1174–1179, (2020).

20. S. K. Nistanaki, C. G. Williams, B. Wigman, J. J. Wong, B. C. Haas, S. Popov, J. Werth, M. S. Sigman, K. N. Houk, H. M. Nelson, Catalytic asymmetric C–H insertion reactions of vinyl carbocations. *Science* **378**, 1085–1091, (2022).

21. A. Aizman, R. Contreras, P. Pérez, Relationship between local electrophilicity and rate coefficients for the hydrolysis of carbenium ions. *Tetrahedron* **61**, 889–895, (2005).

22. D. H. Aue, Dicoordinated carbocations; Rappoport, Z., Stang, P. J., Eds.; John Wiley and Sons: Chichester, pp 105–156, (1997).

23. E. V. Anslyn, D. A. Dougherty, Modern physical organic chemistry, page 88, (2006) ISBN: 978-1-891389-31-3.

24. Z. Li, Z. Zhou, L. Wang, Q. Zhou, C. Tang, Enantioselective reaction of secondary alcohols with phthalimide in the presence of a chiral tri-coordinate phosphorus reagent in Mitsunobu reaction. *Tetrahedron: Asymmetry* **13**, 145–148, (2002).

25. K. Tauber, M. Fuchs, J. H. Sattler, J. Pitzer, D. Pressnitz, D. Koszelewski, K. Faber, J. Pfeffer, T. Haas, W. Kroutil, Artificial multi-enzyme networks for the asymmetric amination of *sec*–alcohols. *Chem. Eur. J.* **19**, 4030–4035, (2013).

26. F. G. Mutti, T. Knaus, N. S. Scrutton, M. Breuer, N. J. Turner, Conversion of alcohols to enantiopure amines through dual–enzyme hydrogen–borrowing cascades. *Science* **349**, 1525–1529, (2015).

27. F.-F. Chen, Y.-Y. Liu, G.-W. Zheng, J.-H. Xu, Asymmetric amination of secondary alcohols by using a redox–neutral two–enzyme cascade. *ChemCatChem* **7**, 3838–3841, (2015).

28. E. Liardo, N. R.-Lombardía, F. Morís, F. Rebolledo, J. G.-Sabín, Hybrid organo- and biocatalytic process for the asymmetric transformation of alcohols into amines in aqueous medium. *ACS Catal.* **7**, 4768−4774, (2017).

29. O. Grossmann, R. Maji, M. H. Aukland, S. Lee, B. List, Catalytic asymmetric additions of enol silanes to *in situ* generated cyclic, aliphatic *N*-acyliminium ions. *Angew. Chem. Int. Ed.* **61**, e20211503, (2022).

30. R. J. Detz, Z. Abiri, R. le Grile. H. Hiemstra, J. H. van Maarseveen, Enantioselective copper-catalysed propargylic substitution: synthetic scope study and application in formal total syntheses of (+)-Anisomycin and (–)-Cytoxazone *Chem. Eur. J.* **17**, 5921–5930, (2011).

31. H. Zhou, H. Y. Bae, M. Leutzsch, J. L. Kennemur, D. Bécart, B. List, The Silicon−Hydrogen exchange reaction: a catalytic σ-bond metathesis approach to the enantioselective synthesis of enol silanes. *J. Am. Chem. Soc.* **142**, 13695–13700, (2020).

32. S. Lee, P. S. J. Kaib, B. List, asymmetric catalysis *via* cyclic, aliphatic oxocarbenium ions. *J. Am. Chem. Soc.* **139**, 2156–2159, (2017).

33. B. Kempf, A. R. Ofial, H. Mayr, π–nucleophilicity in Carbon–Carbon bond-forming reactions. *Acc. Chem. Res.* **36**, 66–77, (2003).

34. H. F. Schaller, A. A. Tishkov, X. Feng, H. Mayr, Direct observation of the ionization step in solvolysis reactions: electrophilicity versus electrofugality of carbocations. *J. Am. Chem. Soc.* **130**, 3012–3022, (2008).

35. D. R. Wallach, J. D. Chisholm, Alkylation of sulfonamides with trichloroacetimidates under thermal conditions. *J. Org. Chem.* **81**, 8035–8042, (2016).

36. A. A. Adhikari, T. Suzuki, R. T. Gilbert, M. R. Linaburg, J. D. Chisholm, Rearrangement of benzylic trichloroacetimidates to benzylic trichloroacetamides. *J. Org. Chem.* **82**, 3982–3989, (2017).

37. K. Ikeuchi, K. Murasawaa, H. Yamada, A simple method for preparation of stainless and highly pure trichloroacetimidate. *Synlett* **30**, 1308–1312 (2019).

38. C. Zhang, G. Zhang, S. Luo, C. Wang, H. Li, Base-catalyzed selective esterification of alcohols with unactivated esters. *Org. Biomol. Chem.* **16**, 8467–8471, (2018).

39. K. Nguyen, V. Nguyen, H. Trau, P. Pham, Organo-photocatalytic C–H bond oxidation: an operationally simple and scalable method to prepare ketones with ambient air. *RSC Adv.* **13**, 7168–7178, (2023).

40. B. M.-Matute, M. Edin, K. Bogár, F. B. Kaynak, J.-E. Bäckvall, Combined ruthenium(II) and lipase catalysis for efficient dynamic kinetic resolution of secondary alcohols. Insight into the racemization mechanism. *J. Am. Chem. Soc.* **127**, 8817–8825, (2005).

41. G. A. B. Vieira, T. L. G. Lemos, M. C. de Mattos, M. da. C. F. de Oliveira, V. M. M. Melo, G. de Gonzalo, V. G.-Fernández, V. Gotor, Chemoenzymatic synthesis of optically active Mugetanol isomers:use of lipases and oxidoreductases in fragrance chemistry. *Tetrahedron:Asymmetry* **20**, 214–219, (2009).

42. B. Wang, X. Tang, J. Liu, H. Yu, *Escherichia coli* BioH: a highly enantioselective and organic solvent tolerant esterase for kinetic resolution of *sec*–alcohols. *Tetrahedron Lett.* **51**, 6360–6364, (2010).

43. A. Vandenberghe, I. E. Markó, F. Lucaccioni, S. Lutts, Enantioselective hydrolysis of racemic 1-phenylethyl acetate by an enzymatic system from fresh vegetables. *Industrial Crops and Products* **42**, 380–385 (2013).

44. A. K. Yudin, L. J. P. Martyn, S. Pandiaraju, J. Zheng, A. Lough, $F_8$-BINOL, an electronically perturbed version of BINOL with remarkable configurational stability. *Org. Lett.* **2**, 41–44, (2000).

45. N. Momiyama, H. Okamoto, J. Kikuchi, T. Korenaga, M. Terada, Perfluorinated aryls in the design of chiral Brønsted acid catalysts: Catalysis of enantioselective [4 + 2] cycloadditions and Ene reactions of imines with alkenes by chiral mono-phosphoric acids with perfluoroaryls. *ACS Catal.* **6**, 1198–1204, (2016).

46. C. Zhu, F. Mandrelli, H. Zho, R. Maji, B. List, Catalytic asymmetric synthesis of unprotected $\beta^2$-amino acids. *J. Am. Chem. Soc.* **143**, 3312–3317, (2021).

47. A. Kinens, S. Balkaitis, O. K. Ahmad, D. W. Piotrowski, E. Suna, Acylative dynamic kinetic resolution of secondary alcohols: tandem catalysis by HyperBTM and Bäckvall's ruthenium complex. *J. Org. Chem.* **86**, 7189−7202, (2021).

48. M.-J. Kim, H. M. Kim, D. Kim, Y. Ahn., J. Park, Dynamic kinetic resolution of secondary alcohols by enzyme–metal combinations in ionic liquid. *Green Chem.* **6**, 471–474, (2004).

49. P. Yuan, J. Chen, J. Zhao, Y. Huang, Enantioselective hydroamidation of enals by trapping of a transient acyl species. *Angew. Chem. Int. Ed.* **57**, 8503–8507, (2018).

50. S. Pal, A. Khatua, M. K. Das, V. Bisai, Concise asymmetric total syntheses of (−)-nuciferol, (−)-nuciferal, and (−)-dihydrocurcumene *via* Rh(I)-catalyzed boronic acid addition. *Tetrahedron Lett.* **65**, 152790, (2021).

51. Y.-G. Chen, B. Shuai, X.-T. Xu, Y.-Q. Li, Q.-L. Yang, H. Qiu, K. Zhang, P. Fang, T.-S. Mei, Nickel-catalyzed enantioselective hydroarylation and hydroalkenylation of styrenes. *J. Am. Chem. Soc.* **141**, 3395–3399, (2019).

52. C. M. Wilson, V. Ganesh, A. Noble, V. K. Aggarwal, Enantiospecific $sp^2$–$sp^3$ coupling of *ortho*- and *para*-phenols with secondary and tertiary Boronic Esters. *Angew. Chem. Int. Ed.* **56**, 16318–16322, (2017).

53. S. Kamble, S. More, C. Rode, Highly selective direct azidation of alcohols over a heterogeneous povidone–phosphotungstic solid acid catalyst. *New J. Chem.* **40**, 10240–10245, (2016).

54. B. McNerney, B. Whittlesey, D. B. Cordes, C. Krempner, A well-defined monomeric aluminum complex as an efficient and general catalyst in the Meerwein–Ponndorf–Verley reduction. *Chem. Eur. J.* **20**, 14959–14964, (2014).

**Acknowledgments:** The authors thank the technicians of our group and the member of our GC, MS, HPLC and NMR service departments. The authors also thank to Oleg Grossmann, Vitor A. F. de Silva and Benjamin Mitschke for their help. We also thank members of the group for internal crowed reviewing.

**Funding:**

Generous support from the Max Planck Society, the Deutsche Forschungsgemeinschaft Cluster of Excellence Ruhr Explores Solvation, RESOLV) and the European Research Council (Early Stage Organocatalysis, ESO) to B.L.

**Author contributions:**

Conceptualization: B.L.

Methodology: V.K.S., C.Z., C.K.D., R.M.

Investigation: V.K.S., C.Z., C.K.D., R.M.

Project administration: B.L.

Supervision: B.L.

NMR: M.L.

DFT: G.B., L.B.

Writing – original draft: V.K.S., C.Z., C.K.D., B.L.

Writing – review & editing: V.K.S., C.Z., C.K.D., B.L.

**Competing interests:** A patent WO2017037141 (A1) filed by the Max-Planck-Institut für Kohlenforschung and B.L. covers the IDPi catalyst class and its applications in asymmetric synthesis. The authors declare no other competing interests.

**Data and materials availability:** All data and synthetic details used in the analysis are available in supporting material.

**Supplementary Materials**

Materials and Methods

Supplementary Text

Figures S1 to S8

Tables S1 to S17

NMR Spectra

HPLC and GC traces

References (*35*-*54*)

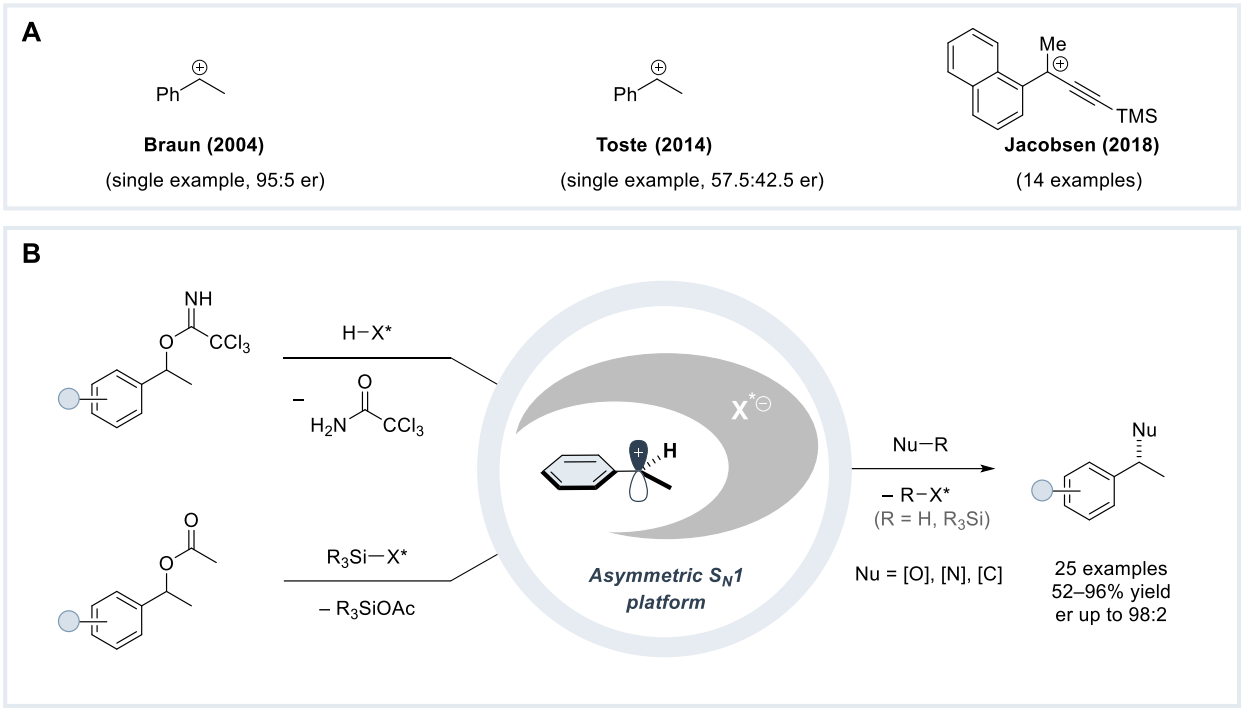
A
Ph
Braun (2004)
(single example, 95:5 er)
Ph
Toste (2014)
(single example, 57.5:42.5 er)
Me
TMS
Jacobsen (2018)
(14 examples)
B
NH
O
CCl3
H–X*
– H2N CCl3
O
O
R3Si–X*
– R3SiOAc
X*⊖
H
Asymmetric SN1 platform
Nu–R
– R–X*
(R = H, R3Si)
Nu = [O], [N], [C]
Nu
25 examples
52–96% yield
er up to 98:2

Figure 1

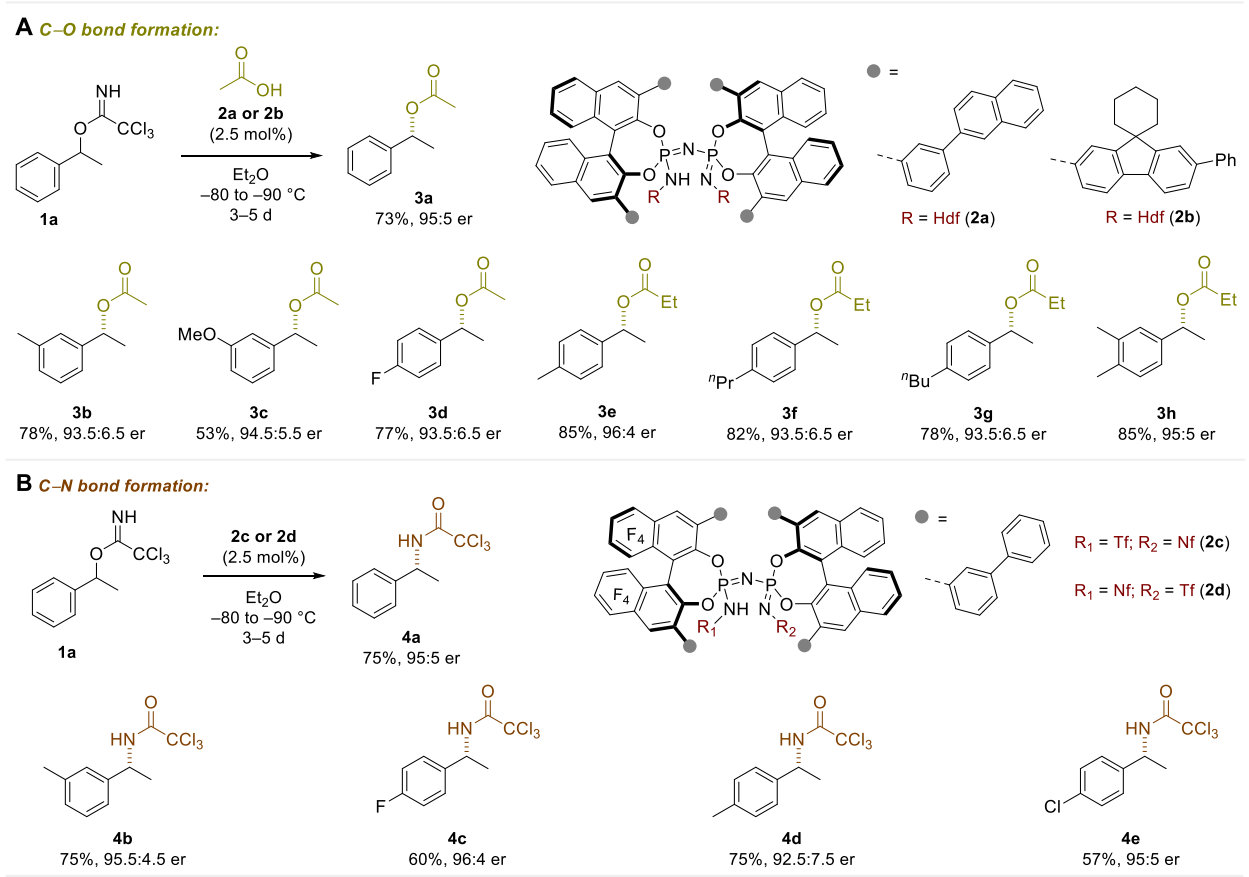
A C–O bond formation:
1a
2a or 2b
(2.5 mol%)
Et2O
–80 to –90 °C
3–5 d
3a
73%, 95:5 er
R = Hdf (2a)
R = Hdf (2b)
3b
78%, 93.5:6.5 er
3c
53%, 94.5:5.5 er
3d
77%, 93.5:6.5 er
3e
85%, 96:4 er
3f
82%, 93.5:6.5 er
3g
78%, 93.5:6.5 er
3h
85%, 95:5 er
B C–N bond formation:
1a
2c or 2d
(2.5 mol%)
Et2O
–80 to –90 °C
3–5 d
4a
75%, 95:5 er
R1 = Tf; R2 = Nf (2c)
R1 = Nf; R2 = Tf (2d)
4b
75%, 95.5:4.5 er
4c
60%, 96:4 er
4d
75%, 92.5:7.5 er
4e
57%, 95:5 er

Figure 2

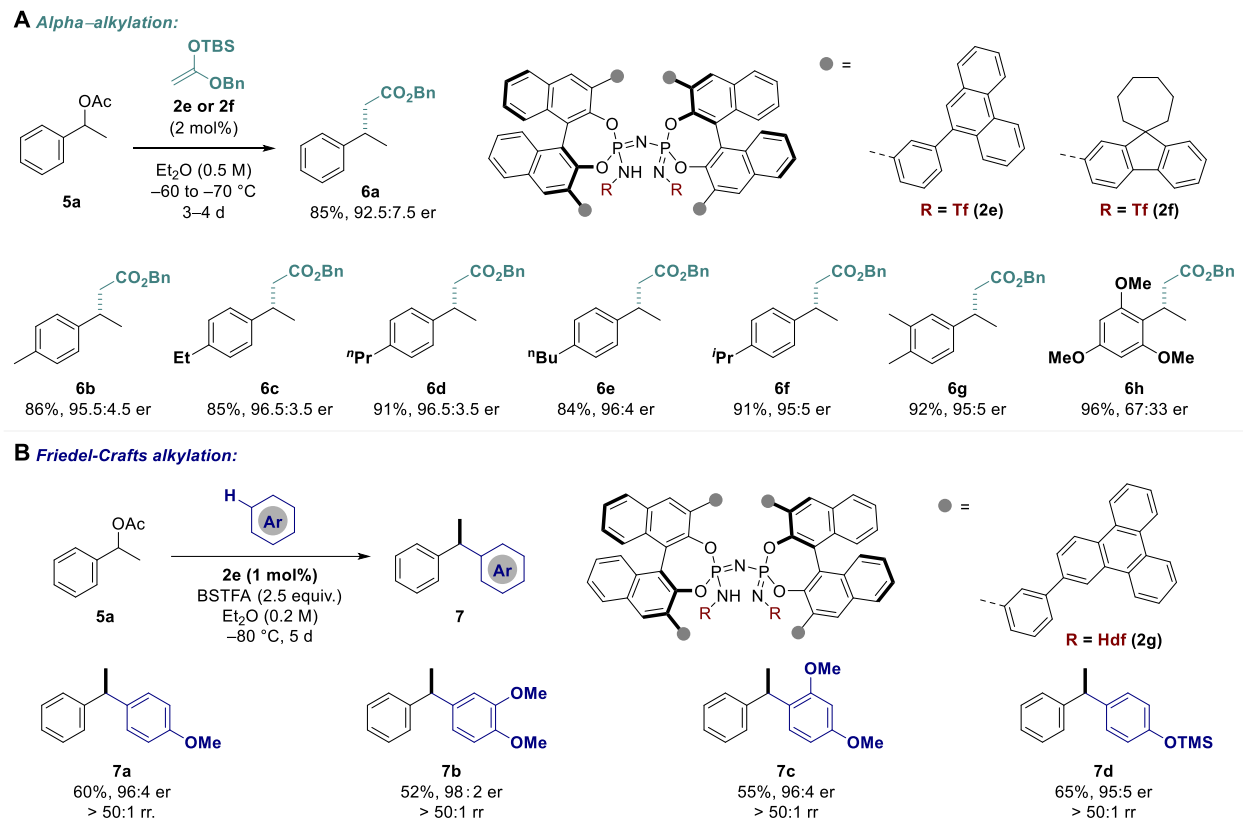
A Alpha–alkylation:
OAc
5a
OTBS
OBn
2e or 2f
(2 mol%)
Et2O (0.5 M)
–60 to –70 °C
3–4 d
CO2Bn
6a
85%, 92.5:7.5 er
R = Tf (2e)
R = Tf (2f)
6b
86%, 95.5:4.5 er
6c
85%, 96.5:3.5 er
6d
91%, 96.5:3.5 er
6e
84%, 96:4 er
6f
91%, 95:5 er
6g
92%, 95:5 er
6h
96%, 67:33 er
B Friedel-Crafts alkylation:
H
Ar
2e (1 mol%)
BSTFA (2.5 equiv.)
Et2O (0.2 M)
–80 °C, 5 d
7
R = Hdf (2g)
OMe
7a
60%, 96:4 er
> 50:1 rr.
7b
52%, 98:2 er
> 50:1 rr
7c
55%, 96:4 er
> 50:1 rr
OTMS
7d
65%, 95:5 er
> 50:1 rr

Figure 3

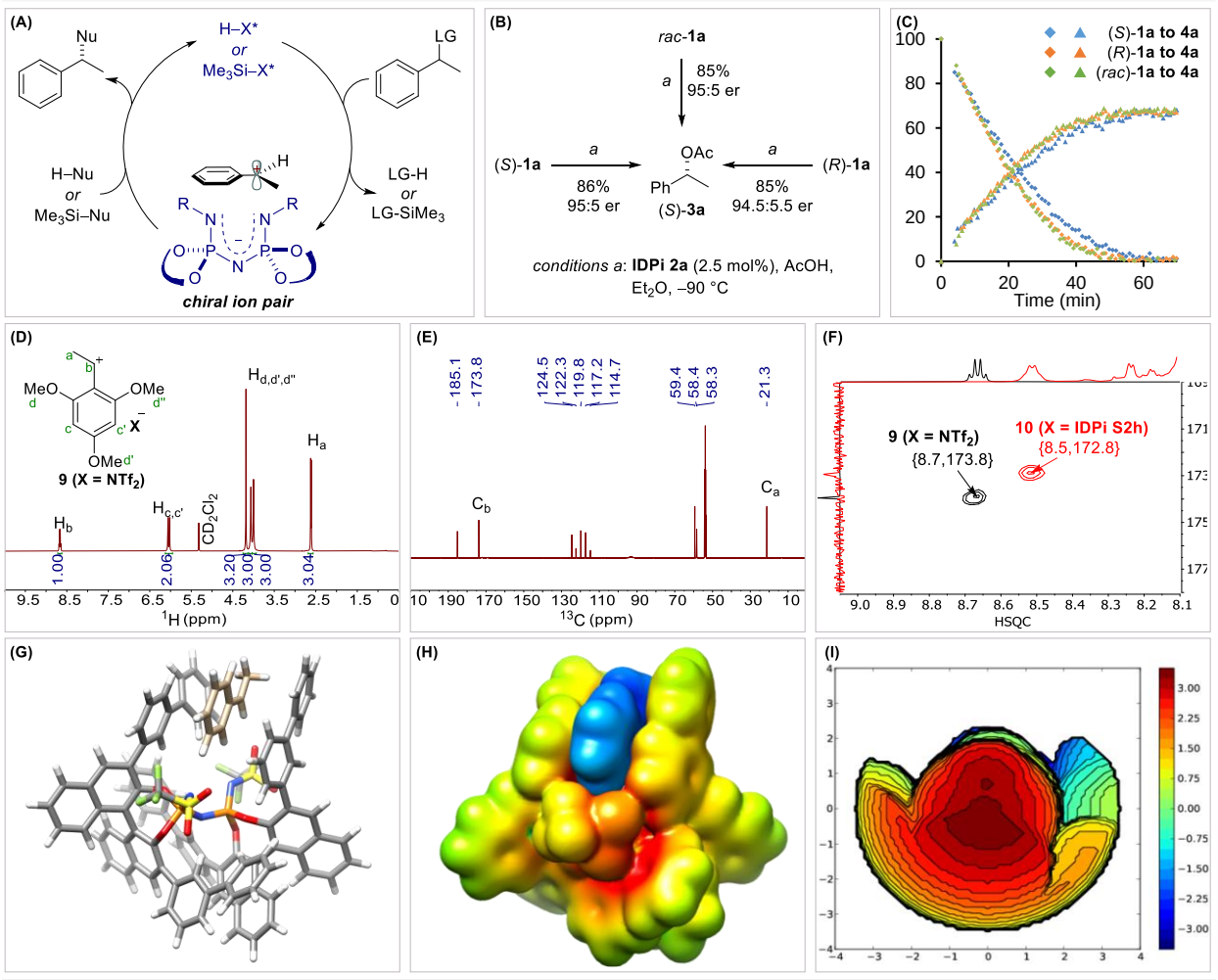
(A)
Nu
H–X*
or
Me3Si–X*
LG
H–Nu
or
Me3Si–Nu
LG-H
or
LG-SiMe3
chiral ion pair
(B)
rac-1a
a
85%
95:5 er
(S)-1a
a
86%
95:5 er
OAc
Ph
(S)-3a
a
85%
94.5:5.5 er
(R)-1a
conditions a: IDPi 2a (2.5 mol%), AcOH,
Et2O, –90 °C
(C)
(S)-1a to 4a
(R)-1a to 4a
(rac)-1a to 4a
Time (min)
(D)
9 (X = NTf2)
Hb
Hc,c'
CD2Cl2
Hd,d',d"
Ha
1H (ppm)
(E)
Cb
Ca
13C (ppm)
(F)
9 (X = NTf2)
{8.7,173.8}
10 (X = IDPi S2h)
{8.5,172.8}
HSQC
(G)
(H)
(I)

Figure 4